Journal for ImmunoTherapy of Cancer

Biomarkers of activity from a phase I study of cergutuzumab amunaleukin in patients with advanced solid tumors

Ignacio Melero ,[1,2] Neeltje Steeghs,[3,4] Ulrik Lassen,[5] Krisztian Homicsko ,[6,7] Josep Tabernero,[8] Marta Cañamero,[9] Andreas Roller ,[10] José Duarte,[10] Eva Rossmann,[10] Galina Babitzki,[11] Nils Grabole,[10] Carl Watson,[12] Christin Habigt,[9] Stefan Evers,[11] David Dejardin,[10] Volker Teichgräber,[11] Jehad Charo [11]

To cite: Melero I, Steeghs N, Lassen U, *et al*. Biomarkers of activity from a phase I study of cergutuzumab amunaleukin in patients with advanced solid tumors. *Journal for ImmunoTherapy of Cancer* 2026;**14**:e012885. doi:10.1136/jitc-2025-012885

► Additional supplemental material is published online only. To view, please visit the journal online (https://doi.org/10.1136/jitc-2025-012885).

Accepted 01 December 2025

For numbered affiliations see end of article.

Correspondence to
Dr Ignacio Melero;
imelero@unav.es

ABSTRACT

Background Cergutuzumab amunaleukin (CA) is an immunocytokine comprising an anticarcinoembryonic antigen (CEA) linked to an interleukin-2 (IL-2) variant. CA does not bind to CD25 (IL-2 receptor α) and was designed to maintain the T and natural killer (NK) cell stimulatory effect, while avoiding stimulating effects on regulatory T cells (Tregs). In mouse models, CA previously demonstrated superior tumor targeting to CEA surface expression-positive (CEA+) tumors and increased CD8+ T cells and NK cell numbers in peripheral blood and tumor tissue when compared with wild-type IL-2. We present biomarker data from the first-in-human, open-label, multicenter, phase I, dose-escalation study investigating CA in patients with metastatic/unresectable CEA+ solid tumors (NCT02004106).

Methods Patients received ascending doses of CA intravenously weekly (qw: 6/10/20 mg) or every 2 weeks (q2w: 10/20/30/40 mg). Flow cytometry determined absolute numbers/mL of CD4+ and CD8+ T cells, NK cells, macrophages/monocytes, Tregs, and B cells and their expression of activation and proliferation markers in circulation. Sequential pretreatment and on-treatment paired tumor biopsies were studied by flow cytometry, multicolor immunohistochemistry, and bulk RNA sequencing. Antitumor activity was used for correlative studies.

Results Biomarker data were collected from 55 patients. After treatment, peripheral blood samples showed increased proliferating NK cells, CD8+ T cells, and CD4+ T cells, without an apparent dose effect. Levels of circulating soluble CD25 increased in patients with intermediate/high CA doses on-treatment; levels of cytokines, such as tumor necrosis factor, also increased with high CA dose levels. On-treatment tumor samples showed increases in total and proliferating CD8+ T cells as well as CD3+ perforin+ T cells but, importantly, not in Tregs. Notably, increases in the ratio of CD8+/CD4+ T cells were more pronounced for qw than for q2w dosing, while programmed death ligand-1-positive CD14+ cells increased, particularly for the q2w schedule. Higher on-treatment circulating levels of cytokines correlated with longer progression-free survival (PFS). Apart from the positive correlation with NK cell density, no other correlations between PFS and infiltrating immune cell populations in the tumor were observed.

Conclusions CA-induced immune pharmacodynamic effects in peripheral blood and in the tumor microenvironment without preferential Treg cell activation in patients with metastatic/unresectable CEA+ solid tumors.

Trial registration number NCT02004106; BP28920

WHAT IS ALREADY KNOWN ON THIS TOPIC

⇒ Cergutuzumab amunaleukin (CA) is a novel immunocytokine comprising an interleukin-2 (IL-2) variant fused to a bivalent carcinoembryonic antigen-targeted antibody, which was designed to maintain the IL-2 stimulatory effect on T and natural killer (NK) cells, while reducing the major limitations of IL-2 as cancer therapy: avoiding stimulatory effects on immunosuppressive regulatory T cells (Tregs); a prolonged half-life to allow more convenient schedules; and an improved safety profile, with less endothelial toxicity and capillary leak, to allow a broader patient population without requiring hospitalization for monitoring and potentially enable use in an outpatient setting.

⇒ In mouse models, CA demonstrated superior targeting, decreased clearance, and increased CD8+ T cells and NK cell levels in peripheral blood and tumor tissue, versus wild-type IL-2.

WHAT THIS STUDY ADDS

⇒ In this biomarker analysis from a phase I study, which included comprehensive plasma biomarkers and longitudinal monitoring of intratumoral changes using serial biopsies, CA had the predicted pharmacodynamic effects, promoting key effector immune cell subsets in peripheral blood and the tumor microenvironment without preferential Treg activation, and triggering inflammation.

HOW THIS STUDY MIGHT AFFECT RESEARCH, PRACTICE OR POLICY

⇒ These biomarker analyses provide pharmacodynamic evidence for the mechanism of action of CA as a selective immune modulator, and the resulting upregulation of immunosuppressive markers such as programmed death-ligand 1 suggests a potential for combination of CA with immune checkpoint inhibition.

BACKGROUND

High-dose recombinant interleukin (IL)-2, aldesleukin, is an approved immunotherapy for metastatic renal cell carcinoma and metastatic melanoma,[1 2] having demonstrated durable objective responses in up to 16% of patients.[3] However, the use of aldesleukin is limited in many patients due to the need for frequent dosing and ensuing severe side effects, which restrict its administration to a hospital setting and often require intensive care.[4 5] The immunologic effects of IL-2 are mediated via IL-2 receptor (IL-2R) binding. Two functional forms of IL-2R have been identified: the trimeric high-affinity IL-2R, composed of IL-2Rα (CD25), IL-2Rβ (CD122), and IL-2Rγ (CD132) subunits (IL-2Rαβγ), and the intermediate affinity IL-2R, composed of IL-2Rβ and IL-2Rγ subunits (IL-2Rβγ). CD4+ CD25+ regulatory T cells (Tregs) constitutively express the high-affinity IL-2R and all activated natural killer (NK), CD8+ and CD4+ T cells where IL-2R is inducible. The intermediate affinity IL-2R is expressed on resting NK cells and a subset of cytotoxic CD8+ T cells without the need for ex vivo activation.[6 7] The expansion of Tregs is an unwanted effect of IL-2-mediated cancer immunotherapy and limits antitumor immune responses.[7–13] To overcome these limitations, and to enhance the antitumor activity of IL-2-based therapy, attention has focused on developing IL-2 antibody-cytokine fusion proteins (immunocytokines) that favor the expansion of cytotoxic T cells rather than Tregs.[6 14] Several IL-2 immunocytokines are in development, mainly in combination with other immune modulators due to a lack of clear and relevant activity of immunocytokine monotherapy,[15 16] but few have progressed beyond phase II trials.[3]

Several additional IL-2-based immunocytokines are being investigated for their potential therapeutic benefits, each with a different mechanism for improving the activity and targeting of IL-2. Molecules such as cergutuzumab amunaleukin (CA) and stroma-targeting FAP-IL2v (simlukafusp alfa)[16] target IL-2 towards molecules that will enable its selective accumulation in the tumor microenvironment (TME). Another approach for tumor targeting is to selectively activate IL-2 within the TME. Examples include WTX-124 and XTX202, which have both demonstrated protease-dependent tumor-selective immune cell activation and clinical activity in phase I studies.[17 18] Active IL-2 mutant or variant (IL-2v) sequences have been created with reduced or no affinity for IL-2Rα (CD25), but with preserved interactions for IL-2Rβγ[19]; these do not selectively stimulate Tregs at low concentrations. More recently, programmed death-ligand 1-IL2v (PD-1-IL2v) (eciskafusp alfa) has been developed, which is a bispecific molecule that targets IL-2 towards immune cells expressing PD-1.[20 21] Treatment with PD-1-IL2v led to significant infiltration of CD8+ T cells in a mouse model of pancreatic neuroendocrine tumors, with tumor regression noted following continued treatment. Moreover, there is evidence that these molecules can reinvigorate exhausted T cells in mice.[22] Similarly, CD8-IL2 is a fusion molecule that targets IL-2 towards intratumoral CD8+ T cells, and was also able to functionally reinvigorate T cells in a preclinical study.[23] As an alternative to IL-2 mutants, polyethylene glycol (PEG)-conjugated IL-2 compounds have been created with masked binding to CD25, and so far have been tested without success in phase III clinical trials in combination with anti-PD-1 checkpoint inhibitors.[24 25]

CA is an immunocytokine composed of a single moiety of IL-2v fused to a bivalent carcinoembryonic antigen (CEA)-targeted antibody that was designed to reduce Treg cell response and off-target receptor binding.[15] CA displays diminished IL-2Rα binding but retains intermediate-binding affinity for IL-2Rβγ expressed on CD8+ T cells, CD4+ T cells, and NK cells.[15] Preclinical data confirmed the superior tumor targeting and reduced clearance of CA compared with wild-type IL-2, with expansion of peripheral and tumor tissue CD8+ T cells and NK cells relative to CD4+ cells and Tregs.[15] An exploratory biodistribution study in patients with solid tumors demonstrated that Zr-89-labeled CA preferentially targeted CEA surface expression-positive (CEA+) tumors, with a trend towards dose-dependent CEA-mediated tumor accumulation.[26]

A first-in-human open-label, multicenter phase I study (NCT02004106) investigated escalating doses of CA in patients with metastatic or unresectable CEA+ solid tumors who had progressed on standard-of-care treatment. The safety, pharmacokinetics, and preliminary antitumor activity of CA have been reported separately.[27] In this study, we report the treatment-associated pharmacodynamic and response biomarker analyses from part II of the study.

METHODS

Study design

The study design of the two-part phase I study (NCT02004106; BP28920) has been described elsewhere (manuscript submitted in parallel),[27] including details of part I. In brief, part II of the study examined multiple ascending doses of CA given intravenously weekly (qw; 6/10/20 mg) or every 2 weeks (q2w; 10/20/30/40 mg), including intrapatient dose escalation, in which the CA dose was increased on the second or third administration (20/25 mg or 20/20/30 mg, respectively). Each cycle was 14 days for q2w dosing and 21 days for every 3 weeks dosing. Patients were observed for dose-limiting toxicities (DLTs) for 21 days, with the first patient in each cohort observed for ≥7 days before further patients were enrolled. Part II used a modified-Continual Reassessment Method with Overdose Control for dose escalation based on DLTs seen at each dose and to establish the maximum tolerated dose (MTD).[28] Dose selection for intrapatient dose escalation was informed by pharmacometric modeling[29 30]; higher dose levels for second or third investigational medicinal product administration were approximated from the observed area under the curve (AUC)

reduction to compensate for the target-mediated drug disposition/antidrug antibody-driven reduction of AUC.

Patients

The study enrolled patients aged ≥18 years with metastatic or unresectable CEA+ solid tumors defined as ≥20% of tumor cell membranes staining with at least moderate intensity by immunohistochemistry (IHC). CEA staining was performed locally with a CEA31 mouse monoclonal IgG1 anti-CD66/CEACAM5 antibody (Cell Marque #760–4594, Ventana Medical Systems, USA) using an in-house validated procedure[26] to determine the cut-off of CEA expression at ≥20% of tumor cell membranes stained with at least moderate intensity. Patients were required to have confirmed disease progression (PD) at baseline per Response Evaluation Criteria in Solid Tumors (RECIST) V.1.1.,[31] measurable disease, and an Eastern Cooperative Oncology Group performance status of 0 or 1. Exclusion criteria included history or evidence of central nervous system primary tumors or metastases, or second malignancy except for a history of non-melanoma skin cancer or cervical carcinoma in situ.

Objectives

The study's primary objectives were to describe the safety profile of different CA dosing regimens, determine the MTD, and define the pharmacokinetics of CA. Secondary objectives were to characterize the pharmacodynamics of single and multiple doses of CA on peripheral blood cells; to obtain preliminary antitumor activity for CA; and to determine changes in biomarkers associated with CA treatment, including proliferation, activation, and infiltration of immune cells and expression of programmed death-ligand 1 (PD-L1). This manuscript presents the detailed biomarker findings, whereas safety, pharmacokinetic, selected pharmacodynamics of peripheral blood cells, and antitumor activity results have been reported separately (Lassen U, Brummelen EMJ, Melero I, et al. Safety, pharmacokinetics, pharmacodynamics, and antitumor activity of cergutuzumab amunaleukin: a phase I study in patients with advanced and/or metastatic solid tumors.).[27]

Outcomes

All pharmacodynamic analyses presented in this manuscript were performed at certified central laboratories. Pharmacodynamic outcomes included the determination of the absolute count of CD4+ and CD8+ T cells, NK cells, macrophages/monocytes, Tregs, and B cells in blood, as well as the expression of activation markers and proliferation markers in tumor biopsies and peripheral blood (Q2 Solutions, Livingston, UK). Cytokines and soluble CD25 (sCD25) were measured in plasma samples using ELLA (R&D Systems, Minneapolis, USA). Tumor biopsies were collected at baseline and on-treatment (cycle 2 day 5 for qw dosing and cycle 1 day 5 for q2w dosing) and were analyzed centrally using flow cytometry and/or IHC (Roche Basel and Roche Penzberg Pathology).[32] IHC was performed on formalin-fixed paraffin-embedded tissue samples. PD-L1 expression was centrally analyzed by IHC in archival or fresh tumor tissue using clone SP142 (Ventana Medical Systems) at CellCarta (formerly known as HistoGeneX (Antwerp, Belgium)). Multicolor IHC was performed as follows: CD3 (2GV6)/PRF (5B10), antigen Kiel 67 (Ki67) (30-9)/CD8 (SP239), forkhead box P3 (FOXP3) (236A/E7) assays were performed, digitized with a DP200 scanner (Ventana Medical Systems) and analyzed using in-house developed imaging algorithms at Roche Innovation Center Munich, Penzberg, Germany,[32] CEA (CEA31) expression was centrally analyzed by IHC using the same protocol as for local assessment, with cells assessed for membrane staining of any intensity (F. Hoffmann-La Roche Ltd Tissue Diagnostics, Tucson, Arizona, USA). Unless indicated otherwise, IHC positivity was assessed in the viable tumor area. Freshly obtained tumor biopsies were also subjected to transcriptome-wide expression profiling by bulk RNA-sequencing (Expression Analysis, a Quintiles company, Durham, North Carolina, USA) after macrodissection of the tumor area.

Statistical analyses

Patients were followed up until PD (according to RECIST V.1.1. or immune-related modified RECIST (mRECIST),[33] whichever occurred later) or until treatment discontinuation due to study withdrawal. Only patients in part II were included in the pharmacodynamic analysis population. No formal statistical hypothesis testing was conducted. All biomarker parameters were listed by the patient, with percent change or absolute change from baseline calculated for each timepoint. Data summaries were tabulated by dose level/regimen and time point, with summary statistics calculated. The analyses presented here are based on a data cut-off date of December 6, 2016.

RESULTS

Patients

55 patients were enrolled in part II of the study, between December 30, 2013 and January 21, 2016. All 55 patients received CA treatment: 31 patients received q2w CA, and 24 received qw CA. Patients ranged in age from 36 to 79 years with a median age of 60 years for those receiving q2w dosing, and 62.5 years for those receiving qw dosing (online supplemental table 2). Patients were mainly male and presented primarily with colon cancer (q2w dosing 44% and qw dosing 57%) or rectal cancer (q2w dosing 19% and qw dosing 14%).

Summary of pharmacodynamics and associations with antitumor activity

Biomarker data were available from all 55 patients who received CA in part II. No patients experienced an objective response per RECIST V.1.1. or mRECIST. The best overall response was disease stabilization. The strongest pharmacodynamic effect observed was the expansion of peripheral immune cells, predominantly NK cells and

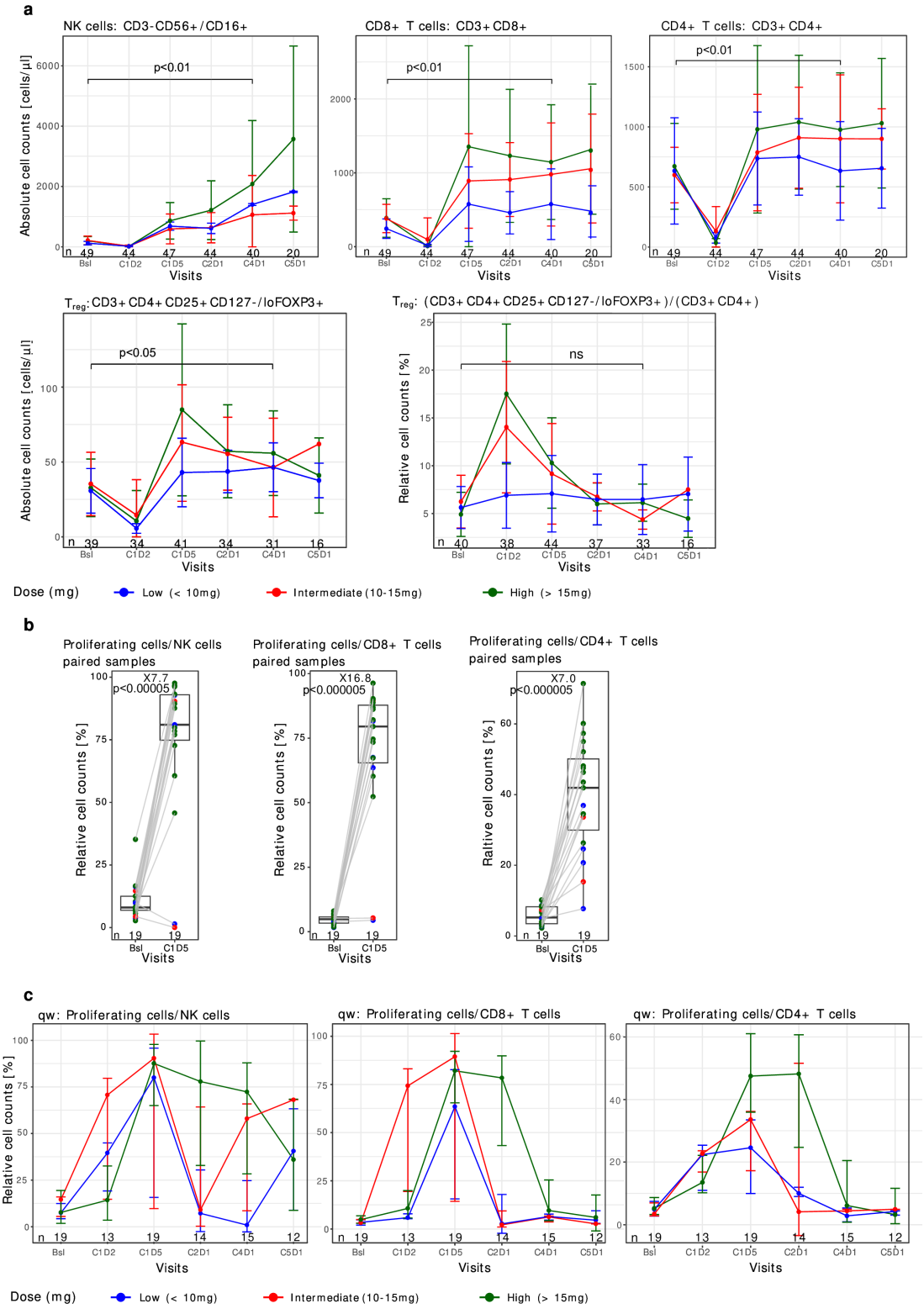

Figure 1 CA strongly expanded NK (CD3−CD56+/CD16+) cells, CD8+ T cells, and to a lesser extent CD4+ T cells in peripheral blood without preferentially expanding Tregs (CD3+CD4+CD25+CD127−/loFOXP3+). Absolute cell count and percentage (%) to parent population of the indicated lymphocyte subpopulation were analyzed by flow cytometry. Data are colored by the level of the dose received on C1D1 for baseline and on-treatment measurements. On dosing days (Bsl/D1), samples were collected prior to dosing. Statistical significance was determined by a Wilcoxon matched-pairs signed rank test. (a) Line graphs showing expansion of lymphocyte subpopulations. Data combined from qw and q2w schedules. Box plots (b) and line graphs (c) showing the percentage of proliferating (Ki67+) cells among NK (CD3−CD56+/CD16+) cells, CD8+ T cells, and CD4+ T cells in peripheral blood following CA treatment (available for qw dosing only). Bsl, baseline; C, cycle; CA, cergutuzumab amunaleukin; D, day; FOXP3, forkhead box P3; Ki67, antigen Kiel 67; CD127−/lo, low or negative expression of CD127; NK, natural killer; ns, not significant; n, number of patient samples; qw, weekly; q2w, every 2 weeks; T_{reg}, regulatory T cells.

CD8+ T cells, but not preferentially Tregs, that seemed to be driven at least in part by lymphocyte proliferation. In the TME, effects were less evident, which might account for the lack of treatment response.

CA biomarkers in peripheral blood

Upon CA treatment, initial lymphopenia was followed by strong and significant expansion of NK, CD8 and to a lesser extent, yet significant, CD4 T cells, including Tregs, was observed in patients' peripheral blood samples that peaked on C1D5 for T cells and on C5D1 for NK cells. An initial transient increase in the percentage of Tregs, probably reflecting preferential redistribution of non-Treg CD4 T cells from the periphery, normalized back to baseline values afterward (figure 1a).[27] No significant changes in the absolute count of macrophages/monocytes and B cells were observed (data not shown). Moreover, increased proportions of proliferating NK cells, CD8+, and CD4+ T cells were seen following CA treatment with a peak at C1D5, without apparent dose-related differences in the tested, rather narrow, dose range. Data were stratified according to dose and dose levels (low dose: <10 mg; intermediate dose: 10 and 15 mg; or high dose: >15 mg; figure 1b and c). These results are in line with previously published data on FAP-IL2v (simlukafusp alfa) that evaluated dose-dependent effects on cell proliferation.[16] The proliferation of these lymphocyte subsets, as detected by Ki67 immunostaining, also peaked on day 5 after the first administration.

Most patients who received intermediate or high CA doses displayed a transient decrease in CD314+ (NK cell receptor G2D (NKG2D+)) NK cells following treatment in cycle 1 day 2 (online supplemental figure 1), similar to the observed change of the overall NK population. Of note, many patients had reduced CD314+NK cells at baseline when compared with healthy donors, but the levels in these patients then normalized after CA treatment in most cases. This decrease in CD314+ NK cells has been previously described in patients with cancer, partly due to high levels of soluble CD314 ligand in serum.[34]

Increased sCD25 levels were observed in plasma following CA qw and q2w dosing (figure 2). In patients who received low doses of CA, sCD25 levels returned to baseline by cycle 2 day 1, whereas levels remained elevated in patients who received intermediate (qw) or high (qw and q2w) CA doses. With qw dosing, not much difference in sCD25 levels was seen between the intermediate and high CA doses; however, with q2w dosing, high CA doses induced higher sCD25 levels than intermediate CA doses. Furthermore, tumor necrosis factor alpha (TNF-α), IL-6, IL-4, and interferon-gamma (IFN-ɣ)-induced protein-10 (IP-10) levels increased in peripheral blood at cycle 1 day 2 and cycle 2 day 2 following treatment with high and intermediate CA doses, both for qw and q2w dosing schedules (figure 3a–d). TNF-α, IL-6, IL-4, and IP-10 levels returned towards baseline 5 days after dosing. In patients treated with low CA doses, minimal increases in IFN-ɣ levels were observed over time (figure 3e). Overall, higher CA dose levels resulted in higher levels of these cytokines.

Baseline and on-treatment peripheral blood levels (corrected for baseline at two landmarks) of TNF-α, IL-6, IL-4, sCD25, IFN-ɣ, and IP-10 correlated with prolonged progression-free survival (PFS) at cycle 2 day 2 and cycle 4 day 2, except IL-6 at the later timepoint (figure 3f). Significant positive correlations (higher soluble protein levels induced on treatment correlated with longer PFS) were observed for circulating IP-10 and sCD25 concentrations. In contrast, at baseline, peripheral blood levels of IL-6, IL-4, sCD25, IFN-ɣ, and IP-10 correlated negatively

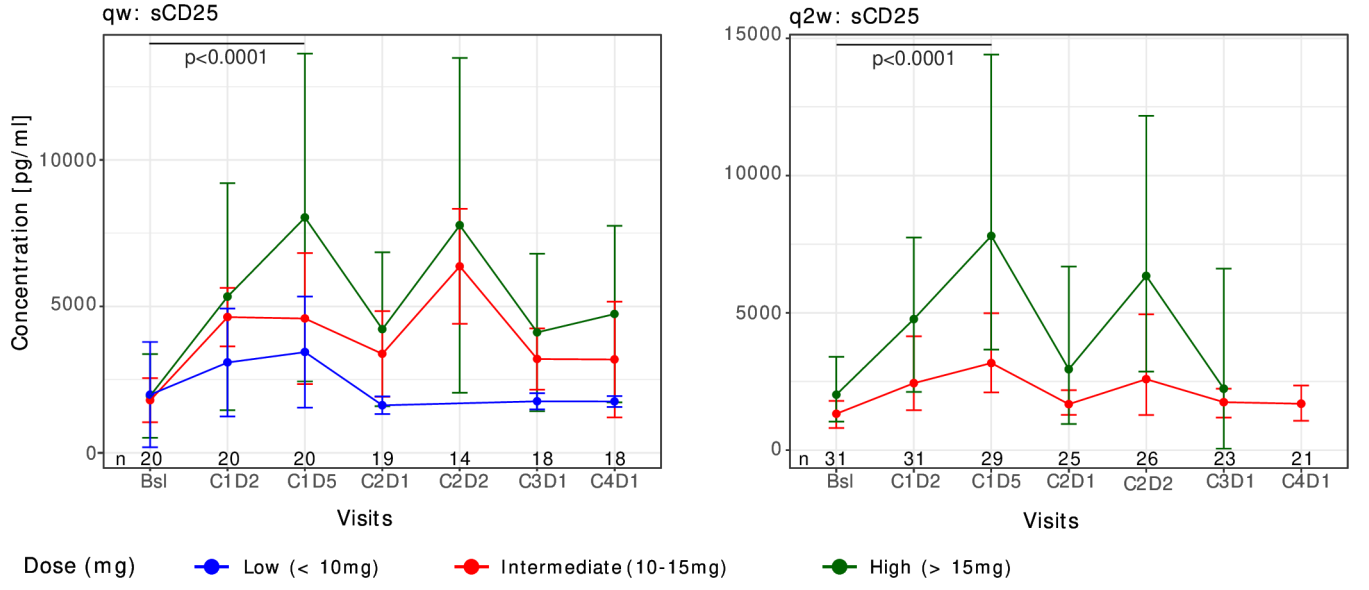

Figure 2 sCD25 levels (pg/mL) in peripheral blood following CA treatment (qw and q2w dosing). Concentrations were measured by ELLA, with data colored by C1D1 dose received. On dosing days (Bsl/D1), samples were collected prior to dosing. Statistical significance was determined by a Wilcoxon matched-pairs signed rank test. Bsl, baseline; C, cycle; CA, cergutuzumab amunaleukin; D, day; qw, weekly; q2w, every 2 weeks; sCD25, soluble CD25.

with PFS. Significant negative correlations (higher baseline soluble protein correlated with shorter PFS) were also observed for circulating IL-4 and sCD25 concentrations.

There were no significant differences in any of the observed peripheral pharmacodynamic effects between samples from patients with or without liver metastasis (online supplemental table 2 and data not shown).

CA biomarkers in tumor samples

In tumor samples, flow cytometry analysis revealed increases in the ratio of CD8+/CD4+ T cells and molecules of equivalent soluble fluorochrome (MESF) of PD-L1+CD14+ cells (macrophages/monocytes) after CA treatment, along with slightly higher CD8+/CD4+ T cell ratios seen following qw dosing (figure 4a), and greater increases in PD-L1+CD14+ MESF observed after q2w dosing (figure 4b).

On-treatment changes in tumor-infiltrating immune cell densities measured by IHC on archived or fresh formalin-fixed paraffin-embedded samples are shown in figure 5. A greater expansion of total and proliferating CD8+ T cells and CD3+ perforin+ cytotoxic T cells was observed after qw versus q2w dosing (figure 5a–c and h). Only minimal expansion was seen for CD3+ T and NK cells, while no expansion of Tregs was evident (figure 5d–f and h). With qw dosing, a change from median PD-L1-negative (0) to median PD-L1-positive (1) was seen in immune cells (figure 5g–h; online supplemental figure 2), and there were no noticeable differences in any of these markers between samples from patients with or without colorectal cancer (CRC) or with or without liver metastasis (online supplemental table 2 and data not shown). No clear relationship was

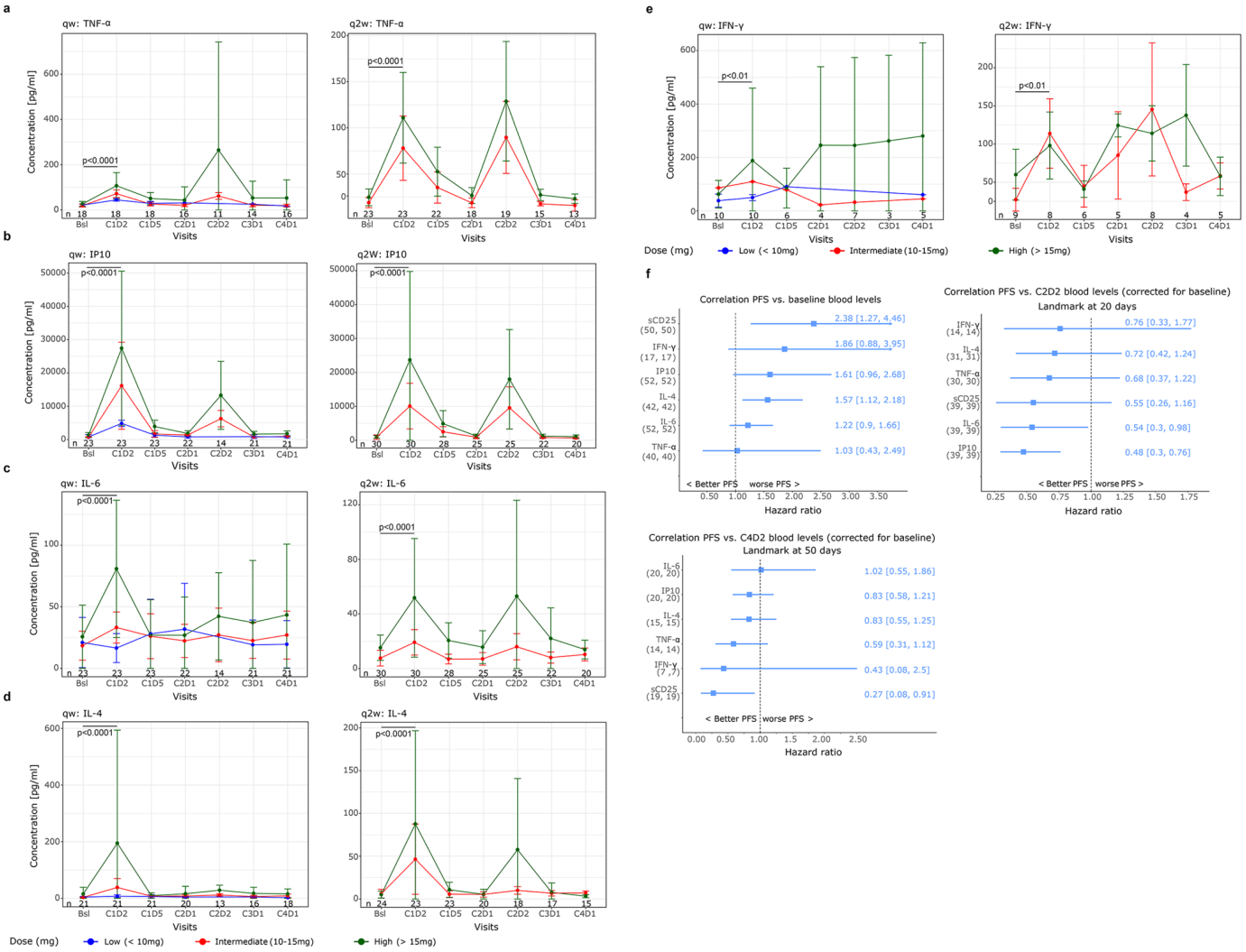

Figure 3 Peripheral blood levels of TNF-α, IP-10, IL-6, IL-4, and IFN-γ. (a–e) Line graphs for individual cytokines. Concentrations were measured by ELLA (pg/mL), with data colored by the level of the received C1D1 dose. On dosing days (Bsl/D1), samples were collected prior to dosing. Statistical significance was determined by a Wilcoxon matched-pairs signed rank test. (f) Forest plots of correlation between PFS and baseline and on-treatment (corrected for baseline) at two landmark levels of sCD25 and indicated cytokines. Data plotted as PFS HR, with error bars representing 95% CIs. Bsl, baseline; C, cycle; D, day; IFN-γ, interferon-γ; IL, interleukin; IP-10, IFN-γ-induced protein-10; PFS, progression-free survival; qw, weekly; q2w, every 2 weeks; sCD25, soluble CD25; TNF-α, tumor necrosis factor-α.

observed between levels of immune cell populations in the tumor after CA treatment (corrected for baseline) and PFS, except for NK cells, which demonstrated a positive correlation with longer PFS (online supplemental figure 3). Central assessment of CEA in tumor tissue indicated that treatment with CA does not affect CEA expression. There was a slight imbalance with higher baseline and on-treatment CEA positivity observed for the qw treated patients (online supplemental figure 4).

Overall, a consistent upregulation of NK cell and cytotoxic T cell gene expression (eg, GNLY and KLR genes) was observed in the entire study cohort between baseline and on-treatment tissue samples when analyzed using bulk RNA sequencing in all patients (figure 6a) and patients with CRC (figure 6b); however, these changes were not significant when corrected for multiple hypothesis testing. Higher expression of gene signatures associated with NK cells was also observed following CA treatment, particularly in biopsies collected from an earlier time point (cycle 1 day 5). Examples of differentially expressed genes and signatures by time point are illustrated in figure 6c–d; the top 50 differentially expressed genes sorted by p value are summarized in online supplemental table 3 (all patients) and online supplemental table 4 (patients with CRC).

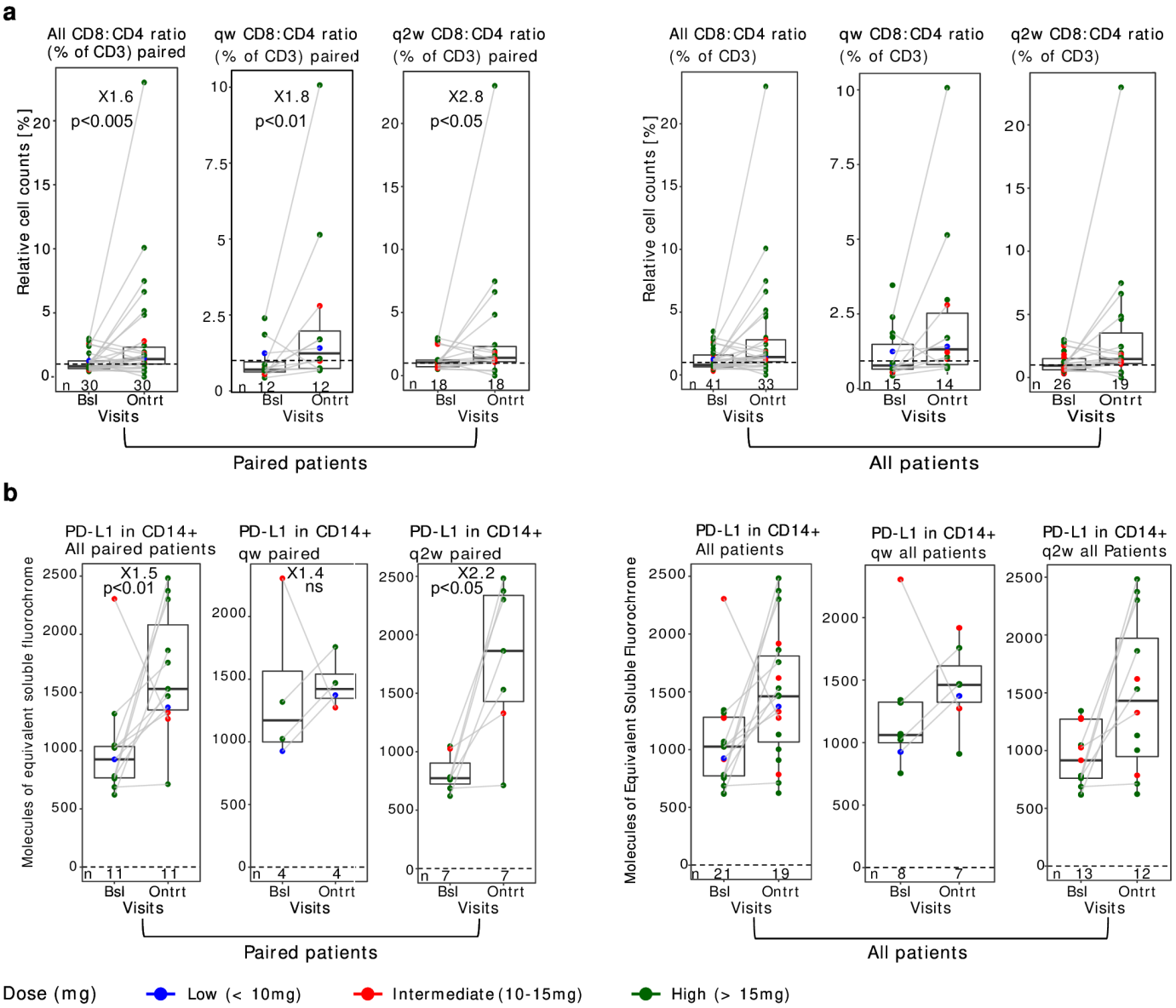

Figure 4 Baseline and on-treatment measurements in tumor samples were determined by flow cytometry: (a) CD8+/CD4+ ratio (calculated from the CD3+ parent population percentage), and (b) PD-L1+ in macrophages/monocytes (CD14+). Lines join data points for paired tumor biopsies. Data are shown for only patients with paired tumor biopsies (left panels) and for all patients (right panels), with colors indicating the C1D1 dose received. Statistical significance was determined by a Wilcoxon matched-pairs signed rank test. Bsl, baseline; ns, not significant; Ontrt, on treatment; PD-L1, programmed death ligand 1; qw, weekly; q2w, every 2 weeks.

DISCUSSION

The expected mechanism of action of CA was to increase the pool of activated and functional NK cells and CD8+ T cells; this was demonstrated in the peripheral blood of patients treated with CA. After treatment, sustained peripheral blood cell expansion was highest for NK cells, followed by CD8+ T cells and CD4+ T cells, but dose effects were not dose-dependent within the tested range. CA was also designed to avoid Treg cell proliferation and, in line with this, no preferential expansion of Tregs in peripheral blood or the TME was observed in this study. CA administration also led to NK and T cell activation in the peripheral blood, as detected by vigorous proliferation and normalization of the CD314 expression.

sCD25 has been described as a marker of IL-2-mediated immune activation, and we observed increased sCD25 in peripheral blood after treatment, indicating a systemic effect of CA. This increase was found to positively correlate with the duration of PFS, which is likely a reflection of the increase in T and NK cell activation. In contrast, higher sCD25 protein level at baseline correlated with lower PFS. This is in line with a previous study where higher sCD25 protein level at baseline correlated with lower overall survival,[35] and suggests sCD25 is an independent negative prognostic factor. This negative prognostic correlation could be explained by higher tumor-promoting inflammation or a higher proportion of Treg abundance or their state of activation. In addition, following treatment with CA, the levels of a number of key cytokines increased in plasma and were found to correlate with longer PFS, again indicating that CA activation of the immune response is associated with better outcome.

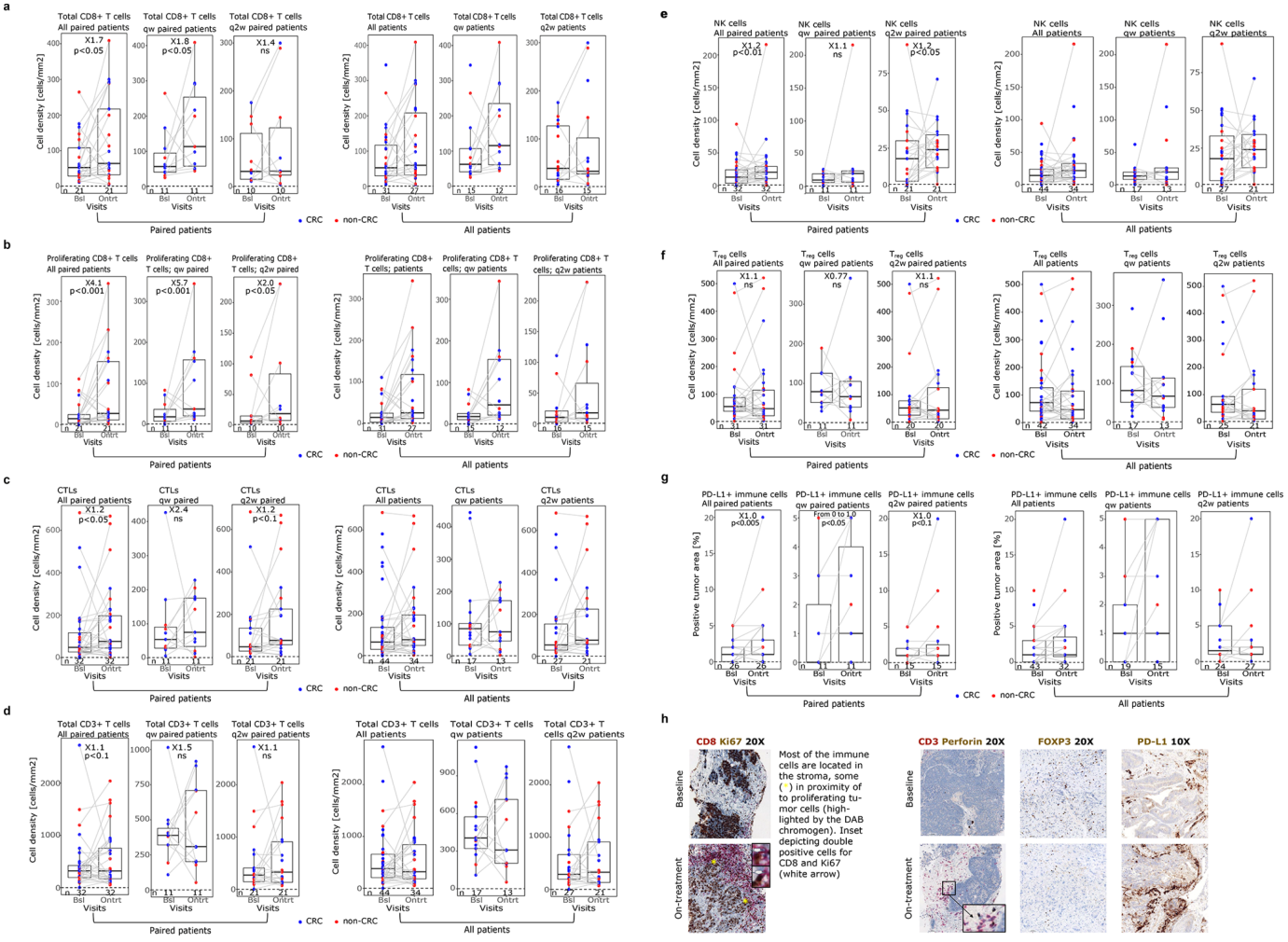

Figure 5 Baseline and on-treatment measurements of tumor-infiltrating immune cells determined by IHC in the tumor area in patients with colorectal versus non-colorectal cancer: (a) total CD8+ T cell densities, (b) proliferating (Ki67+) CD8+ T cell densities, (c) cytotoxic T lymphocyte (CD3+ perforin+) densities, (d) total CD3+ cell densities, (e) NK (CD3− perforin+) cell densities, (f) T_{reg} (FOXP3+) cell densities, (g) percentage of tumor area covered by PD-L1+ immune cells (for a jittered version displaying all data points refer to online supplemental figure 2, (h) representative IHC images of CD8/Ki67, CD3/perforin and FoxP3 staining at 20× magnification and PD-L1 staining at 10× magnification. Lines join data points for paired tumor biopsies. Data are shown for only patients with paired tumor biopsies (left panels) and for all patients (right panels). Statistical significance was determined by a Wilcoxon matched-pairs signed rank test. Bsl, baseline; CRC, colorectal cancer; CTL, cytotoxic T lymphocytes; IHC, immunohistochemistry; NK, natural killer; ns, not significant; Ontrt, on treatment; PD-L1, programmed death-ligand 1; qw, weekly; q2w, every 2 weeks; T_{reg}, regulatory T cells.

IL-6 has been suggested as a prominent driver of cytokine release syndrome;[36 37] in this study, we only observed limited increases in IL-6 levels following CA treatment. In line with this, while IL-2-associated side effects reported in this study such as pyrexia and influenza-like illness are frequent adverse events, cytokine release syndrome did not stand out from the CA safety profile.[27]

In tumor samples, there were trends towards an increase in total and proliferating CD8+ and cytotoxic T cell levels after dosing compared with baseline, indicating an increase in the activation of T cells after treatment. Notably, despite a less consistent increase, on-treatment expansion of NK cells significantly correlated with increased PFS. Treg levels in tumor samples were unaltered or reduced at the time of on-treatment biopsies compared with baseline, which is consistent with the expected mechanism of action.

The impact of CA on immune cell levels, particularly NK cells and activated T cells, is supported by gene signature analyses of tumor tissue. Our findings suggest induction of a lymphocyte-mediated inflammatory phenotype consistent with what has been observed in tumors responsive to IL-2 treatment,[38] with kinetics in line with the potential early role for NK cells in the

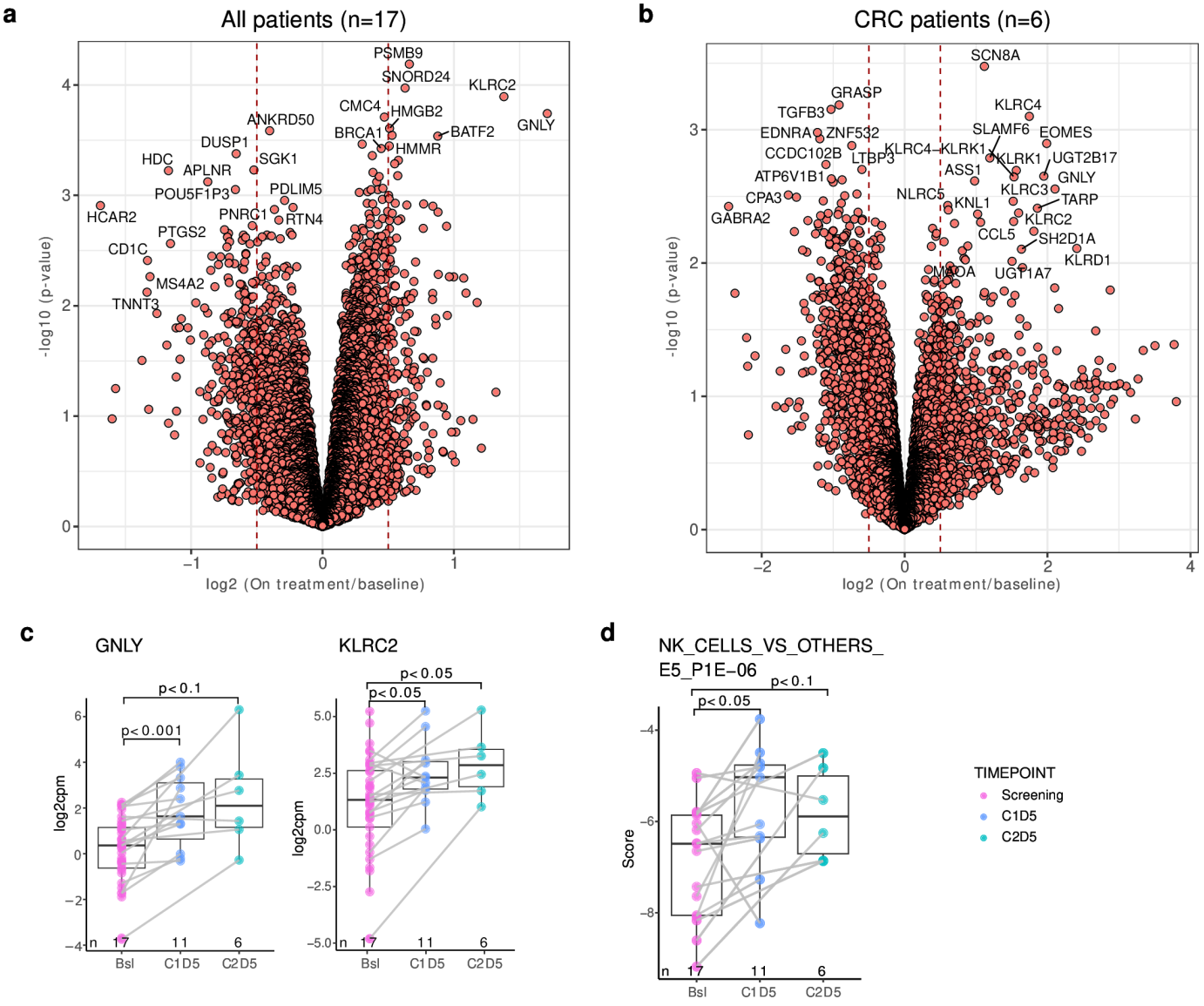

Figure 6 Change in gene expression level from baseline to on-treatment versus p value for: (a) all patients and (b) the CRC cohort. Gene symbols are displayed for differentially expressed genes where the p values are smaller than 0.01. Listings of the top 50 differentially expressed genes by p value can be found in online supplemental table 3 (all patients) and online supplemental table 4 (CRC cohort). Significance was not reached for any genes or signatures when correcting for multiple hypothesis testing using the Benjamini-Hochberg procedure. (c) Differentially expressed genes as log2(cpm) and (d) NK cell-specific signature by timepoint in all patients. Lines join data points for paired tumor biopsies. Baseline samples are shown to the left (pink circles), and on-treatment samples at C1D5 and C2D5 are shown to the right (blue and green circles, respectively). Statistical significance was determined by a Wilcoxon matched-pairs signed rank test. Bsl, baseline; C, cycle; CRC, colorectal cancer; D, day; FOXP3, forkhead box P3; Ki67, antigen Kiel 67; NK, natural killer.

development of an antitumor immune response.[39] The pretreatment composition of the TME might impact the magnitude of the pharmacodynamic effects of CA on the various immune subsets within this microenvironment. However, these results are exploratory in nature and only a limited number of samples were analyzed due to availability, which should be considered when drawing formal conclusions. When correcting for multiple hypothesis testing, no significant differences in the NK cell gene expression patterns were seen. This may be attributed to the low number of tumor samples included in the study.

Currently, one of the IL-2 agents that has progressed furthest is bempegaldesleukin, an IL-2 variant consisting of PEGylated-IL-2 that favors signaling through IL-2Rβ over IL-2Rα. A first in-human biomarker analysis of bempegaldesleukin concluded that on-treatment biopsies demonstrated generalized immune cell increases, including Treg, in the periphery across all doses and cycles but with limited increases or a decrease in Treg levels observed within the TME.[40] In contrast, in the current study, we observed increased immune effector lymphocyte numbers without any apparent Treg expansion in either the periphery or the TME. Bempegaldesleukin was explored in combination with the anti-PD-1 antibody, nivolumab, in the randomized phase III PIVOT IO 001 trial (NCT03635983) in patients with treatment-naïve metastatic melanoma, but the study failed to meet its coprimary endpoints.[24 41]

Alongside the general systemic and intratumoral immune activation observed in this study, we have also observed PD-L1 upregulation in the TME, which might have limited the efficacy of single-agent CA treatment. In the above-mentioned study by Tichet *et al* a similar outcome was observed using a spontaneous tumor mouse model treated with PD-1-IL2v.[21] This study then evaluated the benefit of adding anti-PD-L1 to the PD-1-IL2v treatment regimen. The combination therapy indeed resulted in synergistic efficacy and prolonged survival in the majority of treated mice.[21] Accordingly, in the current study, the increase in PD-L1 levels observed in patients following CA treatment suggests an adaptive resistance mechanism to the therapy, which may be overcome by combining CA with anti-PD-1/PD-L1 therapy.

CONCLUSION

The predicted effects of CA in terms of immune pharmacodynamic effects with no preferential activation of Tregs, but induction of systemic inflammation (sCD25) and proliferation of IL-2Rβγ-expressing effector cells such as NK, CD8+, and CD4+ T cells, were observed when comparing pretreatment and on-treatment patient samples. Notably, in patients who received CA, while there was only limited antitumor cytotoxicity, the inflammatory reaction resulted in the upregulation of immunosuppressive markers such as PD-L1 as a counter-regulatory response, providing a clinical rationale for CA improving efficacy of anti-PD-1/PD-L1 therapy when used in combination. The BP29435 combination study aimed to test this combination hypothesis by evaluating the use of an anti-PD-L1 compound (atezolizumab) with CA treatment in patients with advanced and/or metastatic solid tumors (manuscript in preparation).

Author affiliations
[1]Oncology and Immunology Departments, Clínica Universidad de Navarra, and CIBERONC, Pamplona, Spain
[2]Nuffield Department of Medicine, University of Oxford, Oxford, UK
[3]Department of Medical Oncology, The Netherlands Cancer Institute, Amsterdam, Netherlands
[4]Department of Medical Oncology, University Medical Center Utrecht, Utrecht, Netherlands
[5]Phase 1 Unit, Department of Oncology, Rigshospitalet, Copenhagen University Hospital, Copenhagen, Denmark
[6]Department of Oncology, CHUV, Lausanne, Switzerland
[7]Lausanne Branch, Ludwig Institute for Cancer Research, Lausanne, Switzerland
[8]Medical Oncology Department, Vall d'Hebron University Hospital and Institute of Oncology (VHIO) and CIBERONC, UVic-UCC, IOB-Quiron, Barcelona, Spain
[9]Pharma Research and Early Development, Roche Innovation Center Munich, Penzberg, Germany
[10]Roche Innovation Center, Basel, Switzerland
[11]Roche Innovation Center, Zurich, Switzerland
[12]A4P Consulting Ltd, Sandwich, UK

Acknowledgements We thank the participating patients, their families, research coordinators, and nurses. Flow cytometry panel design and implementation was supervised by Bernhard Reis (F. Hoffmann-La Roche Ltd) and Alistair Watt (Q2 Solutions, Livingston, UK). Medical writing support for the development of this manuscript, under the direction of the authors, was provided by Edward Neale, PhD, of Ashfield MedComms, an Inizio company, and was funded by F. Hoffmann-La Roche Ltd.

Contributors Conception or design of study: IM, JT, SE, VT, JC. Acquisition of data: all authors. Analysis of data: CW, CH, MC, AR, JD, GB, NG, SE, DD, JC. Interpretation of data: all authors. Drafting the article or revising it critically: all authors. Accountability for all aspects of the work: all authors. All authors are guarantors.

Funding This work was supported by F. Hoffmann-La Roche Ltd, which significantly contributed to the study design in collaboration with study investigators, contributed to the collection of data, significantly contributed to the analysis and interpretation of the data in collaboration with study investigators, contributed to the writing of the report with study collaborators, and agreed with the study investigators in the decision to submit the paper for publication. No grant number is applicable.

Competing interests IM has acted in a consulting role to Alligator, AstraZeneca, Bioncotech, Biontech, BMS, Curon, F. Hoffmann-La Roche Ltd., F-STAR, Genmab, Merck-Serono, Pharmamar, and Pioneer Medicines, and received grants from AstraZeneca, Bioncotech, BMS, Genmab and F. Hoffmann-La Roche Ltd. NS provided consultation or attended advisory boards for Boehringer Ingelheim, Bristol-Myers Squibb, Ellipses Pharma, GSK, Incyte. NS received research grants from AbbVie, Actuate Therapeutics, Amgen, Anaveon, Ascendis Pharma, AstraZeneca, Bayer, Blueprint Medicines, Boehringer Ingelheim, Bristol-Myers Squibb, CellCentric, Cogent Biosciences, Cresecendo Biologics, Deciphera, Exelixis, F. Hoffmann-La Roche Ltd., Genentech, Inc., GSK, IDRx, Immunocore, Incyte, Janssen, Kling Biotherapeutics, Lixte, Merck, Merck Sharp & Dohme, Merus, Molecular Partners, Novartis, Pfizer, Revolution Medicines, Sanofi, Seattle Genetics, Taiho, Zentalis. All outside the submitted work, all payment to the Netherlands Cancer Institute. UL has received research support from BMS, F. Hoffmann-La Roche Ltd., GSK, Incyte, Johnson and Johnson, Lilly, Novartis, and Pfizer, and advisory board and speaker's honoraria from AstraZeneca, Bayer and Pfizer. KH has received research support from F. Hoffmann-La Roche Ltd. and MSD, and advisory board and speaker's honoraria from Amgen, BMS, F. Hoffmann-La Roche Ltd., MSD, and Novartis. JT has provided scientific consultancy to Amgen, Bayer, Boehringer Ingelheim, Celgene, Chugai, F. Hoffmann-La Roche Ltd., Genentech, Inc., Lilly, MSD, Merck Serono, Novartis, Sanofi, Symphogen, Taiho, and Takeda. MC, AR, JD, ER, GB, NG, CH, SE, DD, VT, and JC are current or former F. Hoffmann-

La Roche Ltd. shareholders and employees. CW has acted in a consulting role to F. Hoffmann-La Roche Ltd.

Patient consent for publication Not applicable.

Ethics approval The study protocol was approved by the local Ethics Committees/Institutional Review Boards at each center (see online supplemental table 1), and the study was conducted in accordance with the principles of the Declaration of Helsinki and Good Clinical Practice guidelines. All patients provided written informed consent before any study-related procedures.

Provenance and peer review Not commissioned; internally peer reviewed.

Data availability statement Data are available upon reasonable request. For eligible studies, qualified researchers may request access to individual patient level clinical data through a data request platform. At the time of writing this request, the platform is Vivli (https://vivli.org/ourmember/roche/). For up-to-date details on Roche's Global Policy on the Sharing of Clinical Information and how to request access to related clinical study documents, see here: https://go.roche.com/data_sharing. Anonymized records for individual patients across more than one data source external to Roche cannot, and should not, be linked due to a potential increase in risk of patient re-identification.

ORCID iDs
Ignacio Melero https://orcid.org/0000-0002-1360-348X
Krisztian Homicsko https://orcid.org/0000-0003-0912-6198
Andreas Roller https://orcid.org/0000-0001-6335-0962
Jehad Charo https://orcid.org/0000-0002-5409-9160

REFERENCES

1 Fyfe G, Fisher RI, Rosenberg SA, *et al*. Results of treatment of 255 patients with metastatic renal cell carcinoma who received high-dose recombinant interleukin-2 therapy. *J Clin Oncol* 1995;13:688–96.
2 Atkins MB, Lotze MT, Dutcher JP, *et al*. High-dose recombinant interleukin 2 therapy for patients with metastatic melanoma: analysis of 270 patients treated between 1985 and 1993. *J Clin Oncol* 1999;17:2105–16.
3 Sznol M, Rizvi N. Teaching an old dog new tricks: re-engineering IL-2 for immuno-oncology applications. *J Immunother Cancer* 2023;11:e006346.
4 Charych DH, Hoch U, Langowski JL, *et al*. NKTR-214, an Engineered Cytokine with Biased IL2 Receptor Binding, Increased Tumor Exposure, and Marked Efficacy in Mouse Tumor Models. *Clin Cancer Res* 2016;22:680–90.
5 Clinigen, Inc. PROLEUKIN (aldesleukin) prescribing information. 2019. Available: https://www.accessdata.fda.gov/drugsatfda_docs/label/2012/103293s5130lbl.pdf
6 Mortara L, Balza E, Bruno A, *et al*. Anti-cancer Therapies Employing IL-2 Cytokine Tumor Targeting: Contribution of Innate, Adaptive and Immunosuppressive Cells in the Anti-tumor Efficacy. *Front Immunol* 2018;9:2905.
7 Spolski R, Li P, Leonard WJ. Biology and regulation of IL-2: from molecular mechanisms to human therapy. *Nat Rev Immunol* 2018;18:648–59.
8 Maloy KJ, Powrie F. Fueling regulation: IL-2 keeps CD4+ Treg cells fit. *Nat Immunol* 2005;6:1071–2.
9 Fontenot JD, Rasmussen JP, Gavin MA, *et al*. A function for interleukin 2 in Foxp3-expressing regulatory T cells. *Nat Immunol* 2005;6:1142–51.
10 Ahmadzadeh M, Rosenberg SA. IL-2 administration increases CD4+ CD25(hi) Foxp3+ regulatory T cells in cancer patients. *Blood* 2006;107:2409–14.
11 Allen M, Louise Jones J. Jekyll and Hyde: the role of the microenvironment on the progression of cancer. *J Pathol* 2011;223:162–76.
12 Skrombolas D, Frelinger JG. Challenges and developing solutions for increasing the benefits of IL-2 treatment in tumor therapy. *Expert Rev Clin Immunol* 2014;10:207–17.
13 Jiang T, Zhou C, Ren S. Role of IL-2 in cancer immunotherapy. *Oncoimmunology* 2016;5:e1163462.
14 Runbeck E, Crescioli S, Karagiannis SN, *et al*. Utilizing Immunocytokines for Cancer Therapy. *Antibodies (Basel)* 2021;10:10.
15 Klein C, Waldhauer I, Nicolini VG, *et al*. Cergutuzumab amunaleukin (CEA-IL2v), a CEA-targeted IL-2 variant-based immunocytokine for combination cancer immunotherapy: Overcoming limitations of aldesleukin and conventional IL-2-based immunocytokines. *Oncoimmunology* 2017;6:e1277306.
16 Waldhauer I, Gonzalez-Nicolini V, Freimoser-Grundschober A, *et al*. Simlukafusp alfa (FAP-IL2v) immunocytokine is a versatile combination partner for cancer immunotherapy. *MAbs* 2021;13:1913791.
17 Moser JC, Opyrchal M, Rivera IR, *et al*. A phase 1/1b study of the tumor-activated IL-2 prodrug WTX-124 alone or in combination with pembrolizumab in patients with immunotherapy-sensitive locally advanced or metastatic solid tumors. *J Immunother Cancer* 2023;11.
18 Hanna D, Zakharia Y, Goel S, *et al*. XTX202-01, phase 1/2 first-in human study of XTX202, a masked, tumor-activated IL-2βγ, in patients with advanced solid tumors. *J Immunother Cancer* 2023;11.
19 Silva D-A, Yu S, Ulge UY, *et al*. De novo design of potent and selective mimics of IL-2 and IL-15. *Nature* 2019;565:186–91.
20 Codarri Deak L, Nicolini V, Hashimoto M, *et al*. PD-1-cis IL-2R agonism yields better effectors from stem-like CD8+ T cells. *Nature* 2022;610:161–72.
21 Tichet M, Wullschleger S, Chryplewicz A, *et al*. Bispecific PD1-IL2v and anti-PD-L1 break tumor immunity resistance by enhancing stem-like tumor-reactive $CD8^+$ T cells and reprogramming macrophages. *Immunity* 2023;56:162–79.
22 Hashimoto M, Araki K, Cardenas MA, *et al*. PD-1 combination therapy with IL-2 modifies CD8+ T cell exhaustion program. *Nature* 2022;610:173–81.
23 Kaptein P, Slingerland N, Metoikidou C, *et al*. CD8-Targeted IL2 Unleashes Tumor-Specific Immunity in Human Cancer Tissue by Reviving the Dysfunctional T-cell Pool. *Cancer Discov* 2024;14:1226–51.
24 Diab A, Gogas H, Sandhu S, *et al*. Bempegaldesleukin Plus Nivolumab in Untreated Advanced Melanoma: The Open-Label, Phase III PIVOT IO 001 Trial Results. *J Clin Oncol* 2023;41:4756–67.
25 Raeber ME, Sahin D, Karakus U, *et al*. A systematic review of interleukin-2-based immunotherapies in clinical trials for cancer and autoimmune diseases. *EBioMedicine* 2023;90:104539.
26 van Brummelen EMJ, Huisman MC, de Wit-van der Veen LJ, *et al*. ^{89}Zr-labeled CEA-targeted IL-2 variant immunocytokine in patients with solid tumors: CEA-mediated tumor accumulation and role of IL-2 receptor-binding. *Oncotarget* 2018;9:24737–49.
27 Lassen U, Brummelen EMJ, Melero I, *et al*. n.d. Safety, pharmacokinetics, pharmacodynamics, and antitumor activity of cergutuzumab amunaleukin: a phase I study in patients with advanced and/or metastatic solid tumors. *Unpublished Manuscript*.
28 Neuenschwander B, Branson M, Gsponer T. Critical aspects of the Bayesian approach to phase I cancer trials. *Stat Med* 2008;27:2420–39.
29 Ribba B, Grimm HP, Agoram B, *et al*. Methodologies for Quantitative Systems Pharmacology (QSP) Models: Design and Estimation. *CPT Pharmacometrics Syst Pharmacol* 2017;6:496–8.
30 Ribba B, Boetsch C, Nayak T, *et al*. Prediction of the Optimal Dosing Regimen Using a Mathematical Model of Tumor Uptake for Immunocytokine-Based Cancer Immunotherapy. *Clin Cancer Res* 2018;24:3325–33.
31 Eisenhauer EA, Therasse P, Bogaerts J, *et al*. New response evaluation criteria in solid tumours: revised RECIST guideline (version 1.1). *Eur J Cancer* 2009;45:228–47.
32 Brennan L, Brouwer-Visser J, Nüesch E, *et al*. T-Cell Heterogeneity in Baseline Tumor Samples: Implications for Early Clinical Trial Design and Analysis. *Front Immunol* 2022;13:760763.
33 Lencioni R, Llovet JM. Modified RECIST (mRECIST) assessment for hepatocellular carcinoma. *Semin Liver Dis* 2010;30:52–60.
34 Groh V, Wu J, Yee C, *et al*. Tumour-derived soluble MIC ligands impair expression of NKG2D and T-cell activation. *Nature* 2002;419:734–8.
35 Hannani D, Vétizou M, Enot D, *et al*. Anticancer immunotherapy by CTLA-4 blockade: obligatory contribution of IL-2 receptors and negative prognostic impact of soluble CD25. *Cell Res* 2015;25:208–24.

36 Luri-Rey C, Eguren-Santamaria I, Matos I, *et al*. Druggable Targets in Cytokine Release Syndromes. *Clin Cancer Res* 2023;29:4320–2.
37 Leclercq-Cohen G, Steinhoff N, Albertí Servera L, *et al*. Dissecting the Mechanisms Underlying the Cytokine Release Syndrome (CRS) Mediated by T-Cell Bispecific Antibodies. *Clin Cancer Res* 2023;29:4449–63.
38 Weiss GR, Grosh WW, Chianese-Bullock KA, *et al*. Molecular Insights on the Peripheral and Intratumoral Effects of Systemic High-Dose rIL-2 (Aldesleukin) Administration for the Treatment of Metastatic Melanoma. *Clin Cancer Res* 2011;17:7440–50.
39 Kyrysyuk O, Wucherpfennig KW. Designing Cancer Immunotherapies That Engage T Cells and NK Cells. *Annu Rev Immunol* 2023;41:17–38.
40 Bentebibel S-E, Hurwitz ME, Bernatchez C, *et al*. A First-in-Human Study and Biomarker Analysis of NKTR-214, a Novel IL2Rβγ-Biased Cytokine, in Patients with Advanced or Metastatic Solid Tumors. *Cancer Discov* 2019;9:711–21.
41 Khushalani NI, Diab A, Ascierto PA, *et al*. Bempegaldesleukin plus nivolumab in untreated, unresectable or metastatic melanoma: Phase III PIVOT IO 001 study design. *Future Oncol* 2020;16:2165–75.